Synthesis, X-ray Structures, and Spectroscopic Characterization of *cis* and *trans*-bis(O-propyldithiocarbonato)bis(pyridine)nickel(II), *cis* and *trans*-[$Ni(CH_3CH_2CH_2OC(S)S)_2(C_5H_5N)_2$]

Luciana C. Juncal, Evelina G. Ferrer, Patricia A.M. Williams, Roland Boese, C. Gustavo Pozzi, Carlos O. Della Védova, Rosana M. Romano

PII: S0009-2614(22)00154-3
DOI: https://doi.org/10.1016/j.cplett.2022.139487
Reference: CPLETT 139487

To appear in: *Chemical Physics Letters*

Received Date: 31 December 2021
Revised Date: 10 February 2022
Accepted Date: 18 February 2022

Please cite this article as: L.C. Juncal, E.G. Ferrer, P.A.M. Williams, R. Boese, C. Gustavo Pozzi, C.O. Della Védova, R.M. Romano, Synthesis, X-ray Structures, and Spectroscopic Characterization of *cis* and *trans*-bis(O-propyldithiocarbonato)bis(pyridine)nickel(II), *cis* and *trans*-[$Ni(CH_3CH_2CH_2OC(S)S)_2(C_5H_5N)_2$], *Chemical Physics Letters* (2022), doi: https://doi.org/10.1016/j.cplett.2022.139487

Synthesis, X-ray Structures, and Spectroscopic Characterization of *cis* and *trans*-bis(O-propyldithiocarbonato)bis(pyridine)nickel(II), *cis* and *trans*-$[Ni(CH_3CH_2CH_2OC(S)S)_2(C_5H_5N)_2]$

Luciana C. Juncal,[a] Evelina G. Ferrer,[a] Patricia A. M. Williams,[a] Roland Boese,[b] C. Gustavo Pozzi,[a] Carlos O. Della Védova[a] and Rosana M. Romano[a,*]

[a]CEQUINOR (UNLP – CONICET, CCT La Plata, associated with CIC PBA). Departamento de Química, Facultad de Ciencias Exactas, Universidad Nacional de La Plata. Boulevard 120 e/ 60 y 64 N° 1465, La Plata (CP 1900), República Argentina.

[b]Institut für Anorganische Chemie, Universität Duisburg-Essen, Universitätsstr. 5-7, D-45117 Essen, Germany.

In Honor and Memory of Professor Kozo Kuchitsu

Abstract

Single crystals of *cis* and *trans*-bis(O-propyldithiocarbonato)bis(pyridine)nickel(II), *cis* and trans-$[Ni(CH_3CH_2CH_2OC(S)S)_2(C_5H_5N)_2]$, have been prepared and studied using single crystal X-ray diffraction method and IR spectroscopy. The crystal structure of tetracoordinated Ni(II) xanthate complex, bis(O-propyldithiocarbonato)nickel(II), $[Ni(CH_3CH_2CH_2OC(S)S)_2]$, was also determined and compared with the previously reported structure. The existence of a *cis* form for a hexacoordinated species of the $[NiS_4N_2]$ type is infrequent for this family of complexes.

Keywords: Ni(II) complex; O-propyldithiocarbonato complex; Crystal Structure

* Author for correspondence: romano@quimica.unlp.edu.ar

Introduction

Dithiocarbonates are compounds with the −OC(S)S− group in their structures. They were named xanthates after the Greek word "Xanthos" meaning yellowish, golden. Indeed, most xanthate salts are yellow based on their inherent chromophore. They were discovered in 1822 by the Danish organic chemist William Christopher Zeise [1], who was the first to report the synthesis of potassium O-ethyldithiocarbonate (potassium ethylxanthate) by reaction of CS_2, KOH, and ethanol, EtOH. Already at the beginning of the 20th century and later, the versatility of this family of compounds was recognized. Hence, the analytical determination of nickel revealed the necessity for the preparation of stable and reliable potassium O-ethylxanthate [2] In those days, the name xanthate was used as a synonym for the O-ethyl derivative. From then on, their applications increased. Potassium xanthate was used as a soil fumigant [3]; cellulose xanthate [4] was also prepared, and in 1930 a work of significant future impact was published, the use of xanthates to promote the flotation of sphalerite [5] Even nowadays, the applications of compounds containing xanthate in their structure have diversified remarkably. For instance, coordination complexes with a general formula $M(ROC(S)S)_2$, where M is a transition metal cation, were used to prepare nanoparticles and thin films of metal sulfides, with applications in semiconductor materials, heterogeneous catalysis, and photogalvanic cells [6−8]. Another remarkable branch of application for metal coordination complexes containing xanthates is based on their potential pharmacological properties. Relevant studies on their antiviral, antibacterial, antitumoral, and antioxidant properties, among others, have been reported. Metal xanthates are also extensively used as pesticides, corrosion inhibitors, agricultural ingredients, and quite recently, they were considered candidates in therapy for HIV infections and for treating Alzheimer's disease [9−14].

The structural chemistry in the Lewis base adducts of nickel xanthates is rich, and several different coordination geometries were reported in the literature [15,16]. Likewise, the nickel(II) xanthate complexes were reported to form square bidentate ligand complexes $[NiS_4]$ [17] capable of coordinating two additional nitrogen donor species to give either *trans*- or *cis*-$[NiS_4N_2]$ complexes. The reported antecessor found in the literature show a marked abundance in favor of *trans*-$[NiS_4N_2]$ species compared with its geometrical *cis*- isomer. The *cis*- form has a relevant additional property. It suggests the existence of optical isomers, that is, to the formation of non-

superimposable mirror images, opening a field for other extended and more specific applications.

Our interest in this subject was reinforced as a result of a study carried out on species of bis(O-propyldithiocarbonato)nickel(II), [Ni($CH_3CH_2CH_2OC(S)S)_2$], using the facilities of SOLEIL and LNLS Synchrotrons [18]. Additionally to this study, our present investigation reveals another set of data for the previously reported triclinic crystal where both polymorphic forms were obtained at different thermal conditions [19]. Another relevant example also reported that bis(O-ethyldithiocarbonato)nickel(II), and [Ni($CH_3CH_2OC(S)S)_2$], show two polymorphs adopting orthorhombic [20] and triclinic [21] systems. Moreover, the incorporation of this subject allows the merger of knowledge from chemical studies of small molecules, the analysis of transition complexes, and further studies belonging to the discipline of bioinorganic chemistry.

As already mentioned above, the extensive structural data reported for compounds of the [NiS_4N_2] type shows that the *trans* isomer is the one reported in the vast majority of cases. For instance, the *trans* isomer has been found in the structural study for *trans*-bis(O-propyldithiocarbonato)bis(3,5-lutidine)nickel(II), *trans*-[Ni($CH_3CH_2CH_2OC(S)S)_2$-(3,5-$(CH_3)_2C_5H_3N)_2$)] [22], *trans*-bis(O-amyldithiocarbonato)bis(3,5-dimethylpyridine)nickel(II), *trans*-[Ni($CH_3CH_2CH_2CH_2CH_2OC(S)S)_2$-(3,5-$(CH_3)_2C_5H_3N)_2$)] [23], *trans*-bis(O-buthylxanthate)bis(3-chloropyridine)nickel(II), *trans*-[Ni($CH_3CH_2CH_2CH_2OC(S)S)_2$-((3-Cl)$C_5H_4N)_2$)] [24], *trans*-bis(O-propyldithiocarbonato)bis(4-cyanopyridine)nickel(II), *trans*-[Ni($CH_3CH_2CH_2OC(S)S)_2$-((4-CN)$C_5H_4N)_2$)] [25], *trans*-bis(O-butyldithiocarbonato)bis(3,5-dimethylpyridine)nickel(II), *trans*-[Ni($CH_3CH_2CH_2CH_2OC(S)S)_2$-(3,5-$(CH_3)_2C_5H_3N)_2$)] [26], *trans*-bis(O-butyldithiocarbonato)bis(3-ethylpyridine)nickel(II), *trans*-[Ni($CH_3CH_2CH_2CH_2OC(S)S)_2$-((3-$CH_3CH_2$)$C_5H_4N)_2$)] [27], *trans*-bis(O-propyldithiocarbonato)bis(3-chloropyridine)nickel(II), *trans*-Ni[($CH_3CH_2CH_2OC(S)S)_2$-((3-Cl)$C_5H_4N)_2$)] [28], *trans*-bis(O-ethyl dithiocarbonato)bis(isoquinoline)nickel(II), *trans*-[Ni(($CH_3CH_2OC(S)S)_2$-($C_9H_7N)_2$)] [29], *trans*-bis(O-ethyl dithiocarbonato)bis(3,5-dimethylpyridine)nickel(II), *trans*-[Ni($CH_3CH_2OC(S)S)_2$-(3,5-$(CH_3)_2C_5H_3N)_2$)] [30], *trans*-bis(O-butyldithiocarbonato)bis(4-cyanopyridine)nickel(II), *trans*-[Ni($CH_3CH_2CH_2CH_2OC(S)S)_2$-((4-CN)$C_5H_4N)_2$)] [31], and *trans*-bis(O-ethyldithiocarbonato)bis(pyridine-3-carbonitrile)nickel(II), *trans*-[Ni($CH_3CH_2OC(S)S)_2$-((3-CN)$C_5H_4N)_2$)][32]. However, a *cis* isomer was forced to exist using dipyridine as ligand in the preparation of *cis*-bis(O-propyldithiocarbonato)(bipyridine)nickel(II), [Ni($CH_3CH_2CH_2OC(S)S)_2(C_5H_4N)_2$] [33].

However, from the thermodynamic point of view, energy differences of both isomers of $[NiS_4N_2]$ complexes cannot be so distinct to explain this statistical dominance of *trans*-$[NiS_4N_2]$ species observed. Crystal packing forces might also play a role in generating this abundance of *trans*-$[NiS_4N_2]$ complexes in the solid state. Of course, structural differences between the solid state and in solution of a given complex cannot be ruled out according to this assumption.

We also attempted to prepare the $[NiS_4N_2]$ hexacoordinated complex with pyridine, in order to obtain the *cis* form, with further focus on its optic isomerism and, moreover, to acquire one *cis* form accomplishing the long list of *trans* isomers of $[NiS_4N_2]$ species. Following this line of reasoning would suggest finding to break the chiral symmetry for both *cis* enantiomers. It must also be taken into account because this phenomenon cannot be predicted in advance. Such a singularity might be relevant to the origins of life. Recently, a pair of optical isomers formulated as $\{\Delta$ -*cis*-$[Ni(en)_2OAc][ClO_4]\}_n$ and $\{\Lambda$-*cis*-$[Ni(en)_2OAc][ClO_4]\}_n$ (en = ethylendiamine, Ac = acetate) were prepared, isolated and studied [34] by the method discovered by Louis Pasteur in 1848 [35].

Finally, in this work the d^8 new high-spin hexacoordinated paramagnetic *trans*-bis(O-propyldithiocarbonato)bis(pyridine)nickel(II), *trans*-$[Ni(CH_3CH_2CH_2OC(S)S)_2$-$(C_5H_5N)_2)]$ and *cis*-bis(O-propyldithiocarbonato)bis(pyridine)nickel(II), *cis*-$[Ni(CH_3CH_2CH_2OC(S)S)_2$-$(C_5H_5N)_2)]$ (**Figure 1**) have been prepared and structurally and spectroscopically analyzed in the frame of the previous introductory remarks.

Experimental

Sample preparation and purification

Propyl alcohol, $CH_3CH_2CH_2OH$, carbon disulfide, CS_2, potassium hydroxide, KOH, hexahydrated nickel chloride, $NiCl_2.6H_2O$, and pyridine, C_5H_5N, were purchased reagent grade and used without further purification. Solvents as acetone, $CH_3C(O)CH_3$, chloroform, $CHCl_3$, and acetonitrile, CH_3CN, were dried using molecular sieves and distilled subsequently. Potassium O-propyldithiocarbonate (potassium propylxanthate), $CH_3CH_2CH_2OC(S)SK$, was prepared and purified according to literature methods from KOH, CS_2, and the corresponding n-propyl alcohol, $CH_3CH_2CH_2OH$ [36].

$[Ni(CH_3CH_2CH_2OC(S)S)_2]$ was obtained as dark-green crystals by reaction of $CH_3CH_2CH_2OC(S)SK$ with an acetone solution of $NiCl_2.6H_2O$ [18,19].

Cis and *trans*-$[Ni(CH_3(CH_2)_2OC(S)S)_2(C_5H_5N)_2]$ were obtained reacting $[Ni(CH_3CH_2CH_2OC(S)S)_2]$ with pyridine in acetone solution. The reaction mixture was kept under constant stirring at room temperature for two hours. Subsequently, the

reaction mixture was filtered, and a light green translucent solution was obtained. Then, the solvent was slowly evaporated until green crystals were obtained. Their purity was checked through FTIR measurements. This collected sample was subsequently used for single-crystal X-ray diffraction methods and further characterizations.

Computational Chemistry

All quantum chemical calculations were performed using the Gaussian 03 suite of programs [37], using the B3LYP method in combination with a 6-31+G* basis set. Geometry optimization was sought using standard gradient techniques by simultaneous relaxation of all geometrical parameters. The experimental structure determined by crystal X-ray diffraction analysis was taken as starting model, including the point group symmetry of the nickel coordination (C_2 and D_{2h} for the *cis* and *trans* isomers of $[NiS_4N_2]$ complexes, respectively). The calculated vibrational properties correspond to potential energy minima for which no imaginary frequencies were found.

FTIR spectroscopy

FTIR spectra with a resolution of 4 cm^{-1} were recorded at room temperature on a Nexus Thermo Nicolet instrument equipped with an MCTB and a DTGS detector (for the ranges 4000–400 cm^{-1} or 600–100 cm^{-1}, respectively). For each measurement, a total of 32 scans were accumulated. The solid samples were measured in KBr (4000–400 cm^{-1} range) and polyethylene (600–100 cm^{-1} range) pellets.

Crystal data

The determination of the crystal structures was performed at the University of Essen, Germany. The X-ray data were collected on a Bruker D8 diffractometer KAPPA series II with an APEX II area detection system with Bruker AXS APEX 2 Vers.3.0/2009 software [38]. The structures were solved by direct methods using the Bruker AXS SHELXTL Vers 2008/4/(c) 2008 program [39], were completed by Fourier maps, and refined anisotropically for$[Ni(CH_3CH_2CH_2OC(S)S)_2]$ and *cis*-$[Ni(CH_3(CH_2)_2OC(S)S)_2(C_5H_5N)_2]$ and isotropically for *trans*-$[Ni(CH_3(CH_2)_2OC(S)S)_2(C_5H_5N)_2]$ (except H-atoms). The structure analysis, the images, and the study of non-covalent interactions were performed with Mercury 3.1 software [40,41].

Results and discussion

Crystal structure

Crystals for X-ray analysis were obtained after slow evaporation of acetone in the preparation of the complexes. During such procedures, three different types of crystals were analyzed separately, resulting in three different crystal structures corresponding to $[Ni(CH_3CH_2CH_2OC(S)S)_2]$, cis-$[Ni(CH_3CH_2CH_2OC(S)S)_2(C_5H_5N)_2]$, and trans-$[Ni(CH_3CH_2CH_2OC(S)S)_2(C_5H_5N)_2]$ complexes. The crystal structure and packing for the three complexes are presented in **Figure 2** and **Figures S1-S3**.

A summary of the crystallographic data obtained for the three complexes is shown in **Table 1**. The parameters of the collection and processing of data, together with the tables with the atomic coordinates and other geometric parameters, can be found in **Tables S1-S15**. **Tables 2 and 3** show a comparison of bond distances (Å) and angles (°), respectively, found for each complex.

As expected, the C–O distance in the O–C(S) group is lower than in the O–C(C) group for the three structures. This difference is consistent with the mesomeric effect, i.e., the delocalization of π bonds electrons spread over the xanthate chromophore.

It is known that XANES studies link resonances connecting the excitation of core electrons and relatively low energy unoccupied molecular orbitals. Thus, the $[Ni(CH_3CH_2CH_2OC(S)S)_2]$ complex shows resonances at 528.4 and 530.9 eV assigned to O 1s → σ*O–C(C) and O 1s → σ*O–C(S) transitions, respectively. This difference of 2.5 eV is very similar to that found for the resonance signals observed below the ionization potential of C 1s electrons. The corresponding values of 285.0 and 287.6 eV were assigned to C 1s → σ*O–C(C) and C 1s → σ*O–C(S) transitions, giving confidence to the relative positions of both σ*O–C(C) and σ*O–C(S) antibonding orbitals [18].

The same values were also found for both $[Ni(CH_3CH_2CH_2OC(S)S)_2(C_5H_5N)_2]$ isomers. Therefore, the σ O–C(S) molecular orbital was found at about 2.5 eV more stable than the σ O–C(C) molecular orbital for these species. Thus, the mesomeric effect description matches very well the results obtained by XANES measurements for these species. They are predicting a tendency to a double bond character for the O–C(S) bond compared with a single bond character expected in comparison for the O–C(C) bond [42]. In both $[Ni(CH_3CH_2CH_2OC(S)S)_2(C_5H_5N)_2]$ crystal structures, the nickel(II) center is tetra-coordinated by four sulfur atoms. The Ni–S bond distances differ because of the non-equal interactions of sulfur atoms with their environment in the crystal (**Table 2**).

In the $[Ni(CH_3CH_2CH_2OC(S)S)_2]$ crystal structure, the two bidentate xanthate ligands are expected to form essentially equivalent Ni–S bonds. Whereas one xanthate ligand forms

slightly dissimilar Ni−S bonds, i.e. Ni−S(1) 2.226(4) Å is longer than Ni−S(2) of 2.208(4) Å, the second xanthate ligand forms Ni−S bonds of 2.2200(4) Å and 2.2212(4) Å, which are equal length within 3σ. The reason for the slight disparity in the Ni−S distances formed by the first xanthate ligand may be traced to the presence of close intermolecular contacts between the S(1) atom and a symmetry-related Ni atom of 3.275(1) Å (symmetry operation: −x, 1−y, −z). This contact is within the sum of the van der Waals radii for nickel and sulfur of 3.4 Å [43] and may be responsible for the small elongation in the Ni−S(1) bond. Both C–S, and the two O–C(S) and O–C(C) distances present differences almost within the experimental error.

In the *cis*-$[Ni(CH_3CH_2CH_2OC(S)S)_2(C_5H_5N)_2]$ complex, the nickel atom is located on a C_2 symmetry axes, within a hexacoordinated ligand system with C_2 symmetry where the two pyridine ligands are in a *cis* position leading to a *cis*-$[NiS_4N]_2$ coordination (**Figure 1**). The complex units are associated in a three-dimensional arrangement by a variety of supramolecular π···π, C–H···S and C–H···O interactions (**Figure S4**). They might play an important essential role in stabilizing the crystal structure [15,16,44]. The two enantiomeric forms of the complex are depicted in **Figure 3**.

In the *trans*-$[Ni(CH_3CH_2CH_2OC(S)S)_2(C_5H_5N)_2]$ complex, the nickel atom is located in a local approximate (i.e. non-crystallographic) center of inversion and exists within a distorted sphere of *trans*-octahedral coordination, *trans*-S_4N_2. The complex units are associated in a three-dimensional arrangement by a variety of supramolecular C–H···π, C–H···S, C–H···O and S···S interactions (**Figure S4**) which play an essential role in stabilizing the crystal structure [6,25,27,45].

In comparison with the tetracoordinated $[Ni(CH_3CH_2CH_2OC(S)S)_2]$ complex, the hexacoordinated adducts with pyridine produce an increase in the Ni–S interatomic distances,(Table 2) and a decrease of the value of S–Ni–S angle (**Table 3**). These results are in agreement with the reported data found in *cis*-bis(O-propyldithiocarbonato)(bipyridine)nickel(II), $[Ni(CH_3CH_2CH_2OC(S)S)_2(C_5H_4N)_2]$ [33]. Furthermore, the O–C(S) distances for the six coordinated nickel complexes are shorter than the corresponding O–C(C) ones. This fact is again attributable to the higher proportion of π-character in the O–C(S) in comparison with the O–C(C) bonds [17,44,46].

To better understand the nature of the intermolecular interactions present in a $[Ni(CH_3CH_2CH_2OC(S)S)_2]$ crystal, the use of natural bonding orbitals (NBO) results are very useful [47,48]. For such a purpose, NBO analyses were performed using the Gaussian'03 program, with the B3LYP/6-31+G* approximation, taking only two units of

the [Ni($CH_3CH_2CH_2OC(S)S)_2$] complex (**Figure S5**), keeping fixed the intermolecular interactions to be studied. Significant donor-acceptor orbital interactions for the S···Ni and S···S contacts as well as their stabilization energies calculated by means of the second-order perturbation theory (ΔE2), the energy differences between the interacting orbitals, E(j)-E(i), and the values of the Fock integral, F(i,j), are listed in **Table S16**. Likewise, the orbitals involved in these interactions are shown in the **Table**. From this analysis, it can be concluded that both units of the complex contained in the unit cell act reciprocally as donor and acceptor since they present the same type of interactions from one unit to the other. An example of this type of interaction is LP S (5) → σ* Ni(30)–S (31) from unit (a) to unit (b) and LP S(34)→σ* Ni(1)–S(2) from (b) to (a) units. Therefore the resulting structure is doubly stabilized.

IR spectroscopy

Figure 4 shows the FTIR spectra of the *trans* (top) and *cis* (bottom) isomers of [Ni($CH_3CH_2CH_2OC(S)S)_2(C_5H_5N)_2$]. These spectra were compared with antecedents reported in the literature, including among others, pyridine, potassium n-propylxantate [$K^+CH_3CH_2CH_2OC(S)S^-$] [49], the tetracoordinated Ni(II) complex [(Ni($CH_3CH_2CH_2OC(S)S)_2$)] [18], and the hexacoordinated bis-(O-propyldithiocarbonato) bis(4-cyanopyridine)Ni(II) [25], which help to clarify the current assignment. The FTIR vibrational wavenumbers (cm^{-1}) of the hexacoordinated complexes depicted in **Figure 4** are listed in **Table S17**. A complete vibrational study including a preresonance Raman study of the tetracoordinated [Ni($CH_3CH_2CH_2OC(S)S)_2$] complex, was reported elsewhere [18]. Both vibrational data of pyridine and [Ni($CH_3CH_2CH_2OC(S)S)_2$] are also listed in **Table S16** in order to compare these former results with those obtained in the present work.

According to **Figure 1**, the *trans* and *cis*-[Ni($CH_3CH_2CH_2OC(S)S)_2(C_5H_5N)_2$] isomers belong to the D_4h and C_2v symmetry point groups, respectively. Using concepts derived from the group theory, we can expect the *trans* isomer to present a simpler IR spectrum than the *cis* form, especially in the lower wavenumber region of the spectrum, associated with its higher symmetry. It seems evident that some equivalent vibrations will appear duplicated in the spectrum corresponding to the *cis* isomer due to its lower symmetry. The comparison of bands assigned to free pyridine and hexacoordinated [Ni($CH_3CH_2CH_2OC(S)S)_2(C_5HN)_2$] complexes reveals shifts occurring by the formation of the adduct except for the C–N stretching band, assigned at 1584 cm^{-1} in the spectrum of pyridine. This fundamental vibration presents a shift to higher wavenumbers (1597

cm^{-1}) in the hexacoordinated Ni complex evidencing the coordination through the N atom of pyridine and a subsequent redistribution of the electronic density of the cycle. At lower wavenumbers in the FTIR spectra, bands at 603 and 406 cm^{-1}, assigned to in-plane and out-of-plane deformation modes of pyridine, respectively, are shifted to higher energies (*trans* at 630 and 445 cm^{-1}, *cis* at 627 and 442 cm^{-1}) when the $[Ni(CH_3CH_2CH_2OC(S)S)_2(C_5H_5N)_2]$ isomers are formed. These shifts are again indicative of the formation of a complex where the pyridine molecule binds through the nitrogen atom.

Conclusions

The present system formed by Ni(II), the ligand *n*-propylxanthate and pyridine is especially rich in information. Moreover, the hexacoordinated Ni(II) complex with two xanthates and two pyridines appears in its two *cis* and *trans* geometrical isomers. It is the *cis* isomer composed of the two enantiomers, as also evident in its X-ray structure. This versatility in behavior and properties are promising and open future challenges to look also for chiral symmetry breaking of these or related enantiomers belonging to this *cis*-$[NiS_4N_2]$ family.

CCDC Numbers and Supplementary Information

Crystal structure data were deposited with the Cambridge Crystallographic Data Centre (CCDC) for *cis*-bis(O-propyldithiocarbonato)bis(pyridine)nickel(II), *cis*-$Ni(CH_3CH_2CH_2OC(S)S)_2(C_5H_5N)_2]$, Deposition Number 2128960; trans-bis(O-propyldithiocarbonato)bis(pyridine)nickel(II), trans-$Ni(CH_3CH_2CH_2OC(S)S)_2(C5H5N)_2]$, Deposition Number 2128959 and bis(O-propyldithiocarbonato)nickel(II), $[Ni(CH_3CH_2CH_2OC(S)S)_2]$, Deposition Number 2128961.

Supplementary Information: Tables S1-S15 contain crystallographic data of the three crystal structures, Table S16 presents the calculated orbital stabilization between two interacting units of $[Ni(CH_3CH_2CH_2OC(S)S)_2]$ and Table S17 lists the IR wavenumbers of the three complexes. Figures S1-S3 present different views of the crystal packing and Figures S4 and S5 show the interactions and intermolecular contacts for the three complexes. Thermal analysis (TGA and DTA) results of $[Ni(CH_3CH_2CH_2OC(S)S)_2(C_5H_5N)_2]$ under oxygen atmosphere are described and presented in Figure S6.

Acknowledgment

C.O.D.V. and R.M.R. thank the Consejo Nacional de Investigaciones Científicas y Técnicas (CONICET) (PIP 0348 and 0352), the Agencia Nacional de Promoción Científica y Tecnológica (ANPCyT, PICT-2014-3266 and PICT-2018-04355), the Comisión de Investigaciones Científicas de la Provincia de Buenos Aires (CIC), and the Facultad de Ciencias Exactas, UNLP (UNLP-X822 and –X826) for financial support. P.A.M. Williams is research fellow of CICPBA. We are grateful for financial support by the Volkswagen Stiftung. C.O.D.V. acknowledges the Fundación Antorchas, Alexander von Humboldt, DAAD (Deutscher Akademischer Austauschdienst, Germany). He is also indebted to the AvH-Fundación Antorchas and ANPCyT-DAAD for the German-Argentinean cooperation Awards.

References

1. J. Voss, *Journal of Sulfur Chemistry*, 2009, **30**, 167–207.
2. E.D. Campbell, *J. Am. Chem. Soc.,* 1900, **22,** 307-308.
3. E.R. de Ong, *Ind. Eng. Chem*., 1926, **18**, 52-55.
4. G.W. Blanco, *Ind. Eng. Chem*., 1926, **18**, 1257-1259.
5. A.M. Gaudin, *Trans. Am. Inst. Mining Metall. Eng*., 1930, **87,** 417-425.
6. N. Alam, M.S. Hill, G. Kociok-Köhn, M. Zeller, M. Mazhar, K.C. Molloy, *Chem. Mater.,* 2008, **20,** 6157–6162.
7. T. Lutz, A. MacLachlan, A. Sudlow, J. Nelson, M.S. Hill, K.C. Molloy, S.A. Haque*, Phys. Chem. Chem. Phys.* 2012, **14,** 16192–16196.
8. O. Tzhayik, P. Sawant, S. Efrima, E. Kovalev, J.T. Klug, *Langmuir,* 2002, **18,** 3364–3369.
9. E.C. Larsen, J.F. Hatcher, R.M. Adibhatla, *Neuroscience,* 2007, **146**, 946–961.
10. D. de Vos, S.Y. Ho, E.R.T. Tiekink, *Bioinorg. Chem. Appl.,* 2004, **2**, 141–154.
11. W. Friebolin, G. Schilling, M. Zöller, E. Amtmann*, J. Med. Chem.,* 2004, **47**, 2256–2263.
12. V. Gandin, A.P. Fernandes, M.P. Rigobello, B. Dani, F. Sorrentino, F. Tisato, M. Björnstedt, A. Bindoli, A. Sturaro, R. Rella, C. Marzano, *Biochem. Pharmacol.,* 2010, **79,** 90–101.
13. Ö. Güzel, A. Salman, *Bioorg. Med. Chem.*, 2006, **14,** 7804–7815.
14. F. Javed, M. Sirajuddin, S. Ali, N. Khalid, M.N. Tahir, N.A. Shah, Z. Rasheed, M.R. Khan, *Polyhedron,* 2016, **104,** 80–90.
15. E.R.T. Tiekink, I. Haiduc, *Stereochemical Aspects of Metal Xanthate Complexes: Molecular Structures and Supramolecular Self-Assembly*, John Wiley & Sons, Inc., 2005, pp. 127–319.
16. I. Haiduc, R. Micu-Semeniuc, R.F. Semeniuc, M. Campian, A. Fischer, F.T. Edelmann, *Rev. Roum. Chim.*, 2004, **49**, 177–184.
17. M. Franzini, *Z. Kristallogr.* 1963, **118,** 393–403.
18. L.C. Juncal, J. Avila, M.C. Asensio, C.O. Della Védova, R.M. Romano, *Spectrochim. Acta A*, 2017, **180,** 183–192.
19. M.J. Cox, E.R.T. Tiekink, *Z. Kristallogr.* 1996, **211,** 111–113.
20. M. Franzini, *Z. Kristallogr.,* 1963, **118**, 393–403.
21. T. Mizota, Y. Fujii, H. Asahina, *Technol. Reports Yamaguchi Univ*. 1980, **2**, 389–398.
22. N. Sharma, K. Singh, R. Sachar, V.K. Gupta and Rajnikant, *X-ray Struct. Anal. Online,* 2013, **29,** 19-20.
23. K. Singh, N. I. Kour, R. Sachar, V.K. Gupta and V. Rajnikant, *J. Chem. Crystallogr.,* 2012, **42,** 1176–1181.
24. I. Kour, G. Kour, R. Sachar, S. Anthal and R. Kant, *J. Mol. Struct*., 2017, **1128**, 769-774.
25. S. Kapoor, R. Sachar, K. Singh, V.K. Gupta and Rajnikant, *J. Chem. Crystallogr.,* 2012, **42,** 458-463.
26. Neerupama, , R. Sachar, N. Sambyal, K. Kapoor, K. Singh, V.K. Gupta and Rajnikant, *Acta Chim. Slov.* 2013, **60**, 397–402.
27. I. Kaur, K. Singh, G. Kaur, R. Sachar, V.K. Gupta and R. Kant, *J. Crystallogr.,* 2014, 1-6.
28. I. Kour, G. Kour and R. Sachar, *Chem. Science Trans.,* 2014, **3,** 945-952.
29. R.G, Xiong, J.K. Zuo, X.Z. You and X.Y. Huang, *Acta Crist.,* 1996, **C52,** 1157-1159.
30. K. Singh, G. Kour, R. Sharma, R. Sachar, V.K. Gupta, R. Kant, *Eur. Chem. Bull.,* 2014*,* **3,** 463-465.
31. S. Kapoor, R. Sachar, K. Singh,V.K. Gupta, V. Rajnikant, *J. Chem. Crystallogr.,* 2012, **42**, 222-226.
32. S. Kapoor, R. Kour, R. Sachar, R. Kant, V.K. Gupta, K. Kapoor, *Acta Crist. E,* 2012, **68,** m58.
33. K. Singh, S. Kapoor, R. Sachar, V.K. Gupta and Rajnikant, *X-ray Struct. An. On line,* 2012, **28**, 43-44.
34. G.-Ch. Ou, Z.-Z. Li, L. Yuan, X.-Y. Yuan, *Transition Met. Chem.,* 2014, **39**, 393–398.
35. L. Pasteur, *Ann. Chim. Phys.,* 1848, **24**, 442-459.

36. C.C. DeWitt and R.F. Makens, *J. Am. Chem. Soc.*, 1932, **54**, 455–464.
37. M.J. Frisch, G.W. Trucks, H.B. Schlegel, G.E. Scuseria, M.A. Robb, J.R. Cheeseman, J.A.J. Montgomery, T. Vreven, K.N. Kudin, J.C. Burant, J.M. Millam, S.S. Iyengar, J. Tomasi, V. Barone, B. Mennucci, M. Cossi, G. Scalmani, N. Rega, G.A. Petersson, H. Nakatsuji, M. Hada, M. Ehara, K. Toyota, R. Fukuda, J. Hasegawa, M. Ishida, T. Nakajima, Y. Honda, O. Kitao, H. Nakai, M. Klene, X. Li, J.E. Knox, H.P. Hratchian, J.B. Cross, C. Adamo, J. Jaramillo, R. Gomperts, R.E. Stratmann, O. Yazyev, A.J. Austin, R. Cammi, C. Pomelli, J.W. Ochterski, P.Y. Ayala, K. Morokuma, G.A. Voth, P. Salvador, J.J. Dannenberg, V.G. Zakrzewski, S. Dapprich, A.D. Daniels, M.C. Strain, O. Farkas, D.K. Malick, A.D. Rabuck, K.J. Raghavachari, B. Foresman, J.V. Ortiz, Q. Cui, A.G. Baboul, S. Clifford, J. Cioslowski, B.B. Stefanov, G. Liu, A. Liashenko, P. Piskorz, I. Komaromi, R.L. Martin, D.J. Fox, T. Keith, M.A. ALaham, C.Y. Peng, A. Nanayakkara, M. Challacombe, P.M.W. Gill, B. Johnson, W. Chen, M.W. Wong, C. Gonzalez, J.A. Pople, Gaussian 03, Revision B 0.1, 2003..
38. R.H. Blessing, *Acta Crystallogr. A.* 1995, **51**, 33–38.
39. G.M. Sheldrick, *Acta Crystallogr. A.*. 2008, **64(Pt 1)**, 112–122.
40. C.F. Macrae, P.R. Edgington, P. McCabe, E. Pidcock, G.P. Shields, R. Taylor, M. Towler, J. van de Streek, *J. Appl. Crystallogr.* 2006, **39**, 453–457.
41. C.F. Macrae, I.J. Bruno, J.A. Chisholm, P.R. Edgington, P. McCabe, E. Pidcock, L. Rodriguez-Monge, R. Taylor, J. van de Streek, P.A. Wood, *J. Appl. Crystallogr.,* 2008, **41**, 466–470.
42. L.C. Juncal, J. Avila, M.C. Asensio, C.O. Della Védova, R.M. Romano, unpublished results.
43. A. Bondi, van der Waals, *J. Phys. Chem.*, 1964, **68,** 441–451.
44. Z. Trávníček, R. Pastorek, Z. Šindelář, J. Marek, *Transit. Met. Chem.*, 1995, **20,** 67–71.
45. M. Campian, I. Haiduc, E.R.T. Tiekink, *Acta Crystallogr. E*, 2006, **62**, m3516–m3517.
46. Z. Trávníček, R. Pastorek, Z. Šindelář, R. Klička, J. Marek, *Polyhedron.*, 1995, **14**, 3627–3633.
47. F. Weinhold, C.R. Landis, *Valency and bonding : a natural bond orbital donor-acceptor perspective*, Cambridge University Press, Cambridge, UK ; New York, 2005.
48. F. Weinhold, C.R. Landis, *Discovering chemistry with natural bond orbitals,* Wiley, Hoboken, NJ, USA, 2012.
49. L.H. Little, G.W. Poling, J. Leja, *Can. J. Chem.* 1961, **39,** 745–754.

Table 1. Crystallographic Data for $[Ni(CH_3CH_2CH_2OC(S)S)_2]$, *cis*-$[Ni(CH_3CH_2CH_2OC(S)S)_2(C_5H_5N)_2]$ and *trans*- $[Ni(CH_3CH_2CH_2OC(S)S)_2(C_5H_5N)_2]$

	$[Ni(CH_3CH_2CH_2OC(S)S)_2]$	cis-$[Ni(CH_3CH_2CH_2OC(S)S)_2(C_5H_5N)_2]$	trans-$[Ni(CH_3CH_2CH_2OC(S)S)_2(C_5H_5N)_2]$
Formula	$C_8\ H_{14}\ Ni\ O_2\ S_4$	$C_{18}\ H_{24}\ N_2\ Ni\ O_2\ S_4$	$C_{18}\ H_{24}\ N_2\ Ni\ O_2\ S_4$
Formula weight / Da	329.14	487.34	487.34
Density / g cm^{-3} (calc.)	1.707	1.447	1.517
F(000)	340	4064	1016
Temperature / K	100(1)	100(1)	100(1)
crystal size / mm	0.32 x 0.22 x 0.17	0.28 x 0.25 x 0.18	0.13 x 0.11 x 0.01
crystal color	Dark green	Green	Green
Crystal description	Block	Block	Plate
Wavelength / Å	0.71073	0.71073	0.71073
Cryst. system	Triclinic	Orthorhombic	Orthorhombic
Space group	$P\bar{1}$	*Fddd*	$Pna2_1$
Unit cell dimensions			
a / Å	7.4542(5)	14.532(3)	16.9839(10)
b / Å	9.4652(6)	21.130(4)	6.0656(4)
c / Å	9.8106(6)	29.148(4)	20.7121(14)
α / °	73.457(2)	90	90
β / °	86.875(2)	90	90
γ / °	74.910(2)	90	90
Volume / $Å^3$	640.52(7)	8950(3)	2133.7(2)
Z	2	16	4

	$[Ni(CH_3CH_2CH_2OC(S)S)_2]$	cis-$[Ni(CH_3CH_2CH_2OC(S)S)_2(C_5H_5N)_2]$	trans-$[Ni(CH_3CH_2CH_2OC(S)S)_2(C_5H_5N)_2]$
Final R indices [$I > 2\sigma(I)$]	R1 = 0.0259, wR2 = 0.0698	R1 = 0.0205, wR2 = 0.0550	R1 = 0.0818, wR2 = 0.1990
R indices (all data)	R1 = 0.0282, wR2 = 0.0717	R1 = 0.0225, wR2 = 0.0562	R1 = 0.0855, wR2 = 0.2012
Largest diff. peak and hole	0.634 and -0.873 $eÅ^{-3}$	0.431 and -0.202 $eÅ^{-3}$	2.643 and −1.544 $eÅ^{-3}$

Table 2. Selected bond distances (Å) for [Ni($CH_3CH_2CH_2OC(S)S)_2$], *cis*-[Ni($CH_3CH_2CH_2OC(S)S)_2(C_5H_5N)_2$] , and *trans*-[Ni($CH_3CH_2CH_2OC(S)S)_2(C_5H_5N)_2$]

	Ni–S	Ni–N	C–S	(S)C–OC	(S)CO–C
[Ni($CH_3CH_2CH_2OC(S)S)_2$]	2.208 – 2.226	-	1.694 – 1.696	1.304 – 1.308	1.461 – 1.466
[Ni($CH_3CH_2CH_2OC(S)S)_2$][a]	2.204 – 2.223	-	1.682 – 1.694	1.303 – 1.308	1.457 – 1.470
cis-[Ni($CH_3CH_2CH_2OC(S)S)_2(C_5H_5N)_2$]	2.444 – 2.468	2.089	1.696	1.337	1.448
trans-[Ni($CH_3CH_2CH_2OC(S)S)_2(C_5H_5N)_2$]	2.445 – 2.491	2.097 – 2.099	1.696 – 1.705	1.330 – 1.322	1.445 – 1.457

[a] Ref. 19

Table 3. Selected S–Ni–S angles (°) obtained from XRD crystal structures of [Ni($CH_3CH_2CH_2OC(S)S)_2$], *cis*-[Ni($CH_3CH_2CH_2OC(S)S)_2(C_5H_5N)_2$] and *trans*-[Ni($CH_3CH_2CH_2OC(S)S)_2(C_5H_5N)_2$]

[Ni($CH_3CH_2CH_2OC(S)S)_2$]	S(1)–Ni–S(2)	79.32
	S(1)–Ni–S(4)	174.52
	S(1)–Ni–S(3)	99.68
	S(2)–Ni–S(3)	175.05
	S(2)–Ni–S(4)	101.25
	S(3)–Ni–S(4)	79.28
cis-[Ni($CH_3CH_2CH_2OC(S)S)_2(C_5H_5N)_2$]	S(1)–Ni–S(2)	73.38
	S(1)–Ni–S(4)	97.28
	S(3)–Ni–S(2)	97.28
	S(1)–Ni–S(3)	166.88
	S(2)–Ni–S(4)	91.56
	S(3)–Ni–S(4)	73.38
trans-[Ni($CH_3CH_2CH_2OC(S)S)_2(C_5H_5N)_2$]	S(1)–Ni–S(2)	73.62
	S(1)–Ni–S(4)	178.95
	S(1)–Ni–S(3)	107.86
	S(2)–Ni–S(3)	178.34
	S(2)–Ni–S(4)	105.37
	S(3)–Ni–S(4)	73.16

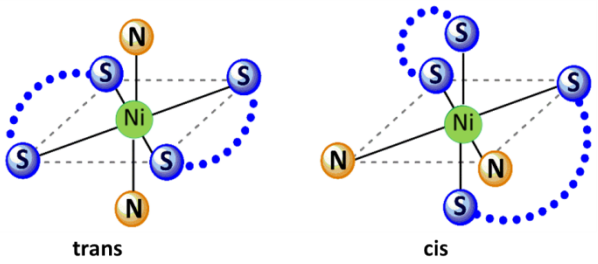

Figure 1. Hexacoordinated *trans*- and *cis*- complexes of the type $[NiS_4N_2]$.

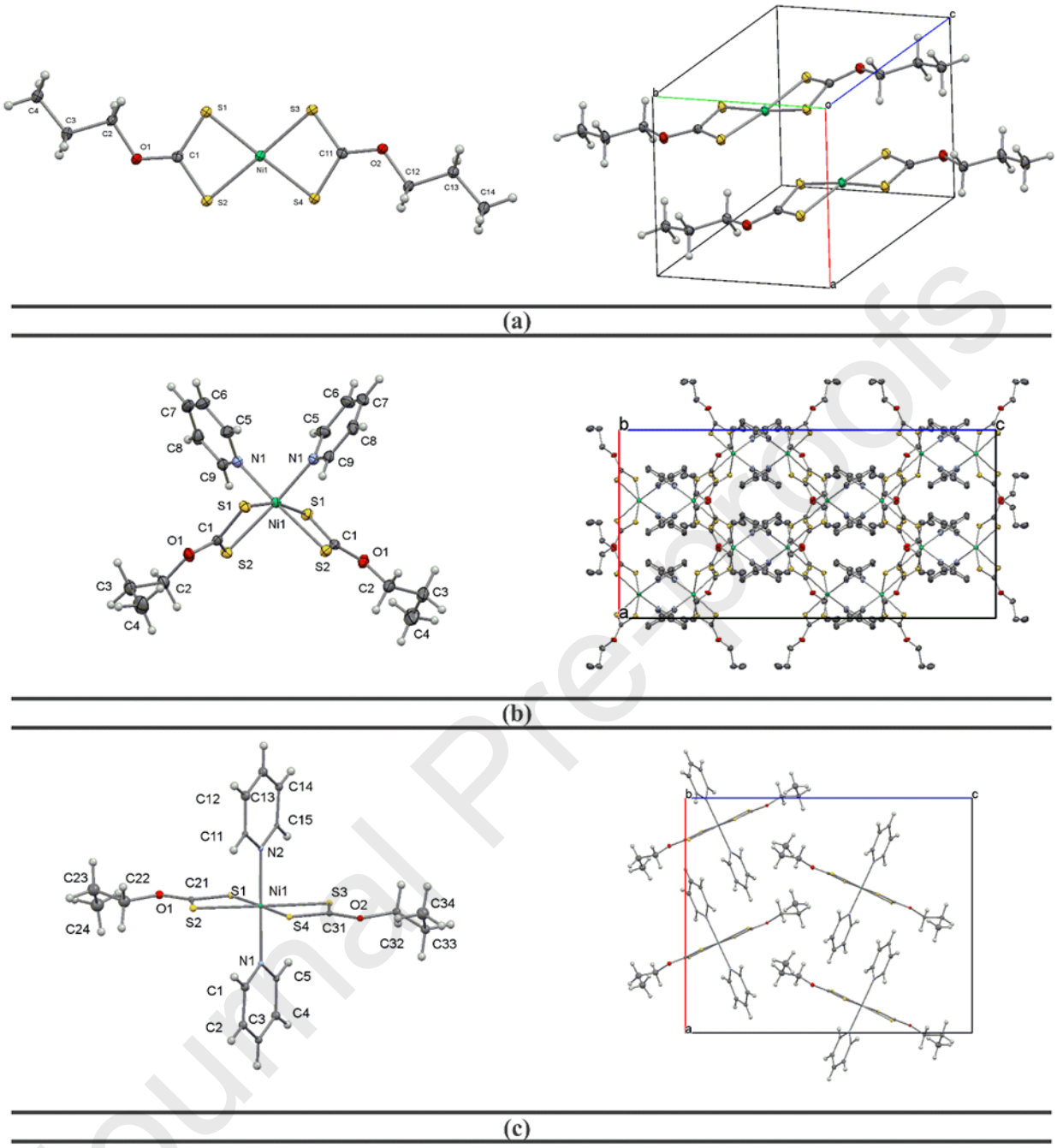

Figure 2. ORTEP X-ray structure with numerical notation scheme and unit cell for (a) $[Ni(CH_3CH_2CH_2OC(S)S)_2]$, (b) *cis*-$[Ni(CH_3CH_2CH_2OC(S)S)_2(C_5H_5N)_2]$ and (c) *trans*-$[Ni(CH_3CH_2CH_2OC(S)S)_2(C_5H_5N)_2]$. Ellipsoidal displacements of atoms other than hydrogen are plotted with a probability level of 50%.

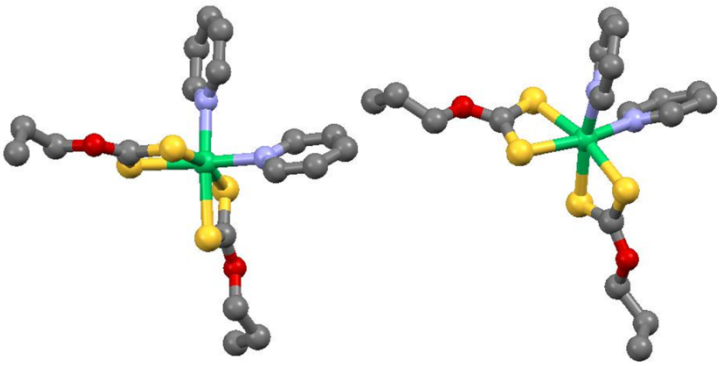

Figure 3. The enantiomers of *cis*-[Ni($CH_3CH_2CH_2OC(S)S)_2(C_5H_5N)_2$] in the racemic complex (hydrogen atoms were omitted for clarity).

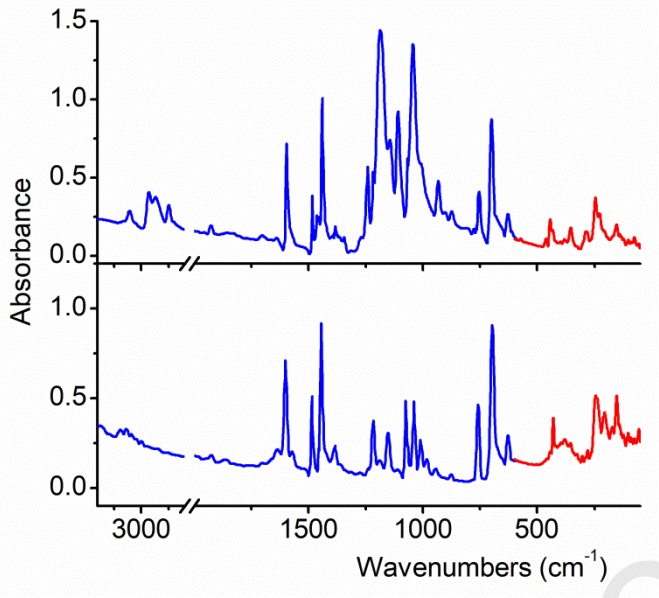

Figure 4. FTIR spectra (blue trace between 3200 and 600 cm^{-1} and red trace between 600 and 50 cm^{-1}) of the two forms of $[Ni(CH_3CH_2CH_2OC(S)S)_2(C_5H_5N)_2]$ assigned to the *trans* (top) and *cis* (bottom) isomer respectively.

Graphical Abstract

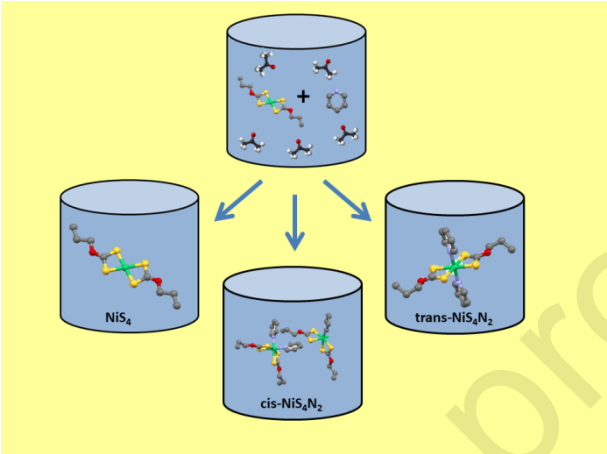

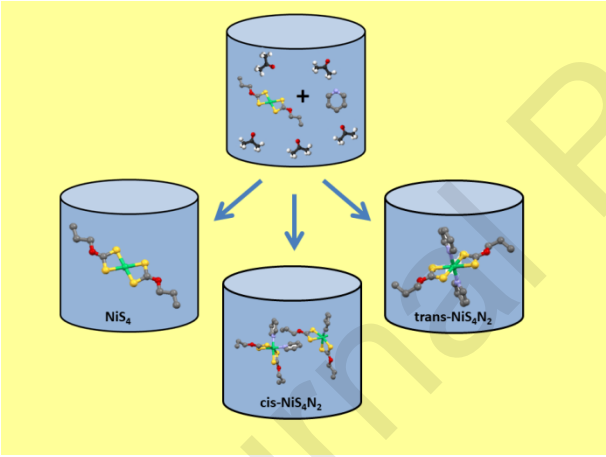

- $[Ni(CH_3CH_2CH_2OC(S)S)_2(C_5H_5N)_2]$ complex have been prepared
- Trans and cis isomers of $[Ni(CH_3CH_2CH_2OC(S)S)_2]$ were determined by X-ray diffraction
- The *cis* structure found for this complex is infrequent for these type of species

CRediT author statement

Luciana C. Juncal: Investigation, Validation
Evelina G. Ferrer: Investigation
Patricia A. M. Williams: Investigation
Roland Boese: Methodology, Investigation, Formal analysis
C. Gustavo Pozzi: Formal analysis

Carlos O. Della Védova: Conceptualization, Writing, Funding acquisition
Rosana M. Romano: Conceptualization, Writing, Supervision, Funding acquisition

Declaration of interests

☒ The authors declare that they have no known competing financial interests or personal relationships that could have appeared to influence the work reported in this paper.

☐The authors declare the following financial interests/personal relationships which may be considered as potential competing interests: